3 August 1962, Volume 137, Number 3527 **SCIENCE**

Crystalline Structure and Surface Reactivity

Atomistic models are unique tools for dealing with the chemical and physical properties of surfaces.

Harry C. Gatos

It has been known for some time that crystalline structure and crystallographic orientation play important roles in various surface phenomena—adsorption, catalysis, and metallographic etching, to name but a few The influence of surface structure is manifested also in the phenomena of nucleation and crystal growth, in the work function, and in other properties which are not generally considered to be directly associated with surface behavior. In many instances, orientation effects have been attributed to differences in packing (surface atom density) or in thermodynamic stability.

The role of orientation in surface behavior is a specific aspect of the overall influence of crystalline structure on surface reactivity. In considering an ideally periodic lattice, it is apparent that the abrupt termination of the lattice at the surface must result in unique crystalline configurations of atoms whose behavior must also reflect the presence of unaccommodated chemical bonds. Quantum mechanical or statistical treatments represent one approach to the problem of crystalline surfaces. Such treatments have shown that additional electron energy levels—as Tamm states (*1*),—are associated with the surface. One theoretical treatment of semiconductor surfaces (*2*) has been quite successful; it served to a large extent as the essential background in the development of the transistor. In general, however, quantum or statistical treatments of surfaces are in a primitive state of development (*3*) and can be employed only sparingly in the interpretation of surface behavior or in predicting surface characteristics.

It is frequently profitable, however, to consider the surface atoms as individual entities bonded to the lattice but with fewer near-neighbor bonds than atoms in the interior of the crystal. In the case of metals, it is difficult to visualize the chemical bonds on the basis of the classical bond orbital model, since the number of nearest neighbors is relatively high (12 in the case of face-centered structures) and the metallic bond is a resonating one (that is, not localized). In covalent crystals on the other hand, where the number of nearest neighbors is relatively small (four in the case of diamond-type materials) and where the bonds are highly directional, one can visualize the surface as a plane of atoms possessing dangling bonds.

In a comprehensive treatment of surface behavior based on chemical bonding it is necessary to take into account possible rearrangements of the surface atoms and the fact that surface contamination is, for all practical purposes, implicit in dangling bonds. Present knowledge of surface-atom rearrangements is very limited, and although such rearrangements cannot be ignored, they must be considered for the present to be second-order effects. The contamination problem can be eliminated only under extreme and elaborate conditions (*4*), but it can perhaps be minimized through moderate experimental control.

A solid surface may be considered to be a giant lattice defect. Conversely, internal lattice defects, particularly line defects such as dislocations, can be treated as free surfaces. It appears that strains associated with lattice defects are not as important as the bonding configuration of the "surface" atoms in determining chemical reactivity. The pronounced influence of chemical bonding on the properties of solids, including surface characteristics, is perhaps most strikingly illustrated by recalling the differences between the diamond and the graphite forms of carbon. No attempt is made here, in this article, however, to discuss the surface properties as they are affected by crystalline structure in various allotropic forms. My purpose is to examine the surface behavior and the behavior of lattice defects in the light of an atomistic or chemical bonding approach. The discussion is limited to primarily covalent materials. In the context of chemical bonding concepts, metallic surfaces represent a far more complex case than the covalent surfaces.

Orientation Effects

Differences in chemical reactivity among surfaces of different orientation are not commonly observed. This is not surprising, since the corresponding surface free energies are not marked (*5*) and become imperceptible in fast reactions. Moreover, when the rate-determining step of a reaction does not

---

The author is associate head of the Solid State Division, Lincoln Laboratory, Massachusetts Institute of Technology, Lexington.

Table 1. Correlation between the density of free surface bonds, the work function (*12*), and the dissolution rates of germanium in O_2-saturated H_2O (*17*).

Orientation	Free bonds (per cm^2)	Relative free-bond density	Relative work function	Relative dissolution rates
$\{100\}$	1.25×10^{15}	1.00	1.00	1.00
$\{110\}$	8.83×10^{14}	0.71	0.95	0.89
$\{111\}$	7.22×10^{14}	.58	.93	.62

involve the direct participation of the surface atoms, the surface structure is of no significance (*6*). The influence of orientation is most pronounced in relatively slow reactions where the surface atoms participate in the rate-determining step, so that kinetic considerations become more pertinent than thermodynamic considerations. Although I do not attempt a comprehensive classification of orientation effects, I can distinguish the following general types of surface reactions:

1) Reactions with liquid or gaseous ambients in which the resulting products do not remain on the surface. Metallographic etching, employed for many years for the study of polycrystalline materials (*7*), is essentially based on the preferential reaction of the differently oriented grains with the etchant (liquid or gaseous)—a reaction which results in the development of the individual grains and of the corresponding grain boundaries (Fig. 1).

Under suitable conditions, etching of single crystals leads to the formation of well-defined etch figures which reflect the crystallographic symmetry of the etched surface (Fig. 2). Etch figures have been used for some time for determining the orientation of crystals and for studying the thermodynamic stability of the various crystallographic planes (equilibrium or steady-state forms) (*8*).

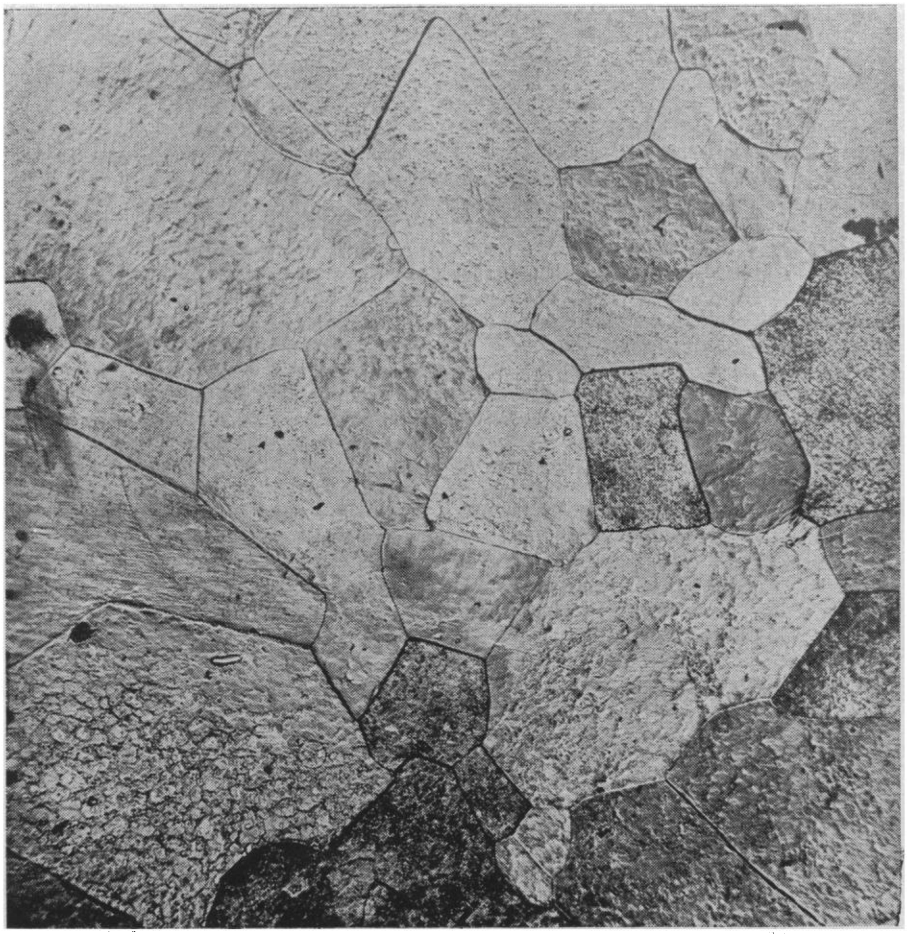

Fig. 1. Polycrystalline sample of copper etched in 5*N* HNO_3. The appearance of the individual grains results from differences in their chemical reactivity brought about by differences in orientation. The reactivity of the grain boundaries, which are essentially defect structures, also differs from that of the corresponding grains (× 50).

2) Crystal growth and thermal etching. These are essentially reciprocal processes which depend upon nucleation phenomena at the surface. Perhaps the earliest indication of the role of crystalline orientation in surface phenomena was the observation that naturally occurring or artificially grown single crystals develop certain crystallographic planes. Although crystal habit does not appear at first to be a surface effect, it is undoubtedly influenced by the fact that the probability of nucleation is markedly affected by the geometric arrangement of the surface atoms. Thus, single crystals grown without seeding grow not at random but in one or possibly more preferred orientations (Fig. 3). The role of surface orientation in crystal growth is frequently manifested indirectly: impurities adsorbed preferentially on certain crystallographic planes may serve as nucleation centers or as inhibitors of crystal growth (*9*).

The formation of surface etch patterns by heating at elevated temperatures in a vacuum or in gaseous ambients—thermal etching—proceeds either through direct sublimation or through the intermediate formation of volatile compounds. In either case, the nucleation as well as the propagation processes of thermal etching are strongly dependent upon crystallographic orientation. Thermal etching usually results in the development of the individual grains but, under suitable conditions, may lead to the formation of thermal etch figures. Although thermal etching is in many respects similar to ordinary etching, it is better suited to the study of details of the etching process under near-equilibrium conditions.

3) Formation of epitaxial layers. It has been known for some time that material *A* grown as a thin layer on substrate *B* frequently acquires the structure of material *B*; for example, gold and a number of other metals deposited on the $\{100\}$ surface of rock salt take up the orientation of the substrate crystal (*10*). It has also been observed that dislocations in the substrate can be propagated into epitaxially grown material (*11*) (Fig. 4). Epitaxial growth is closely related to the normal

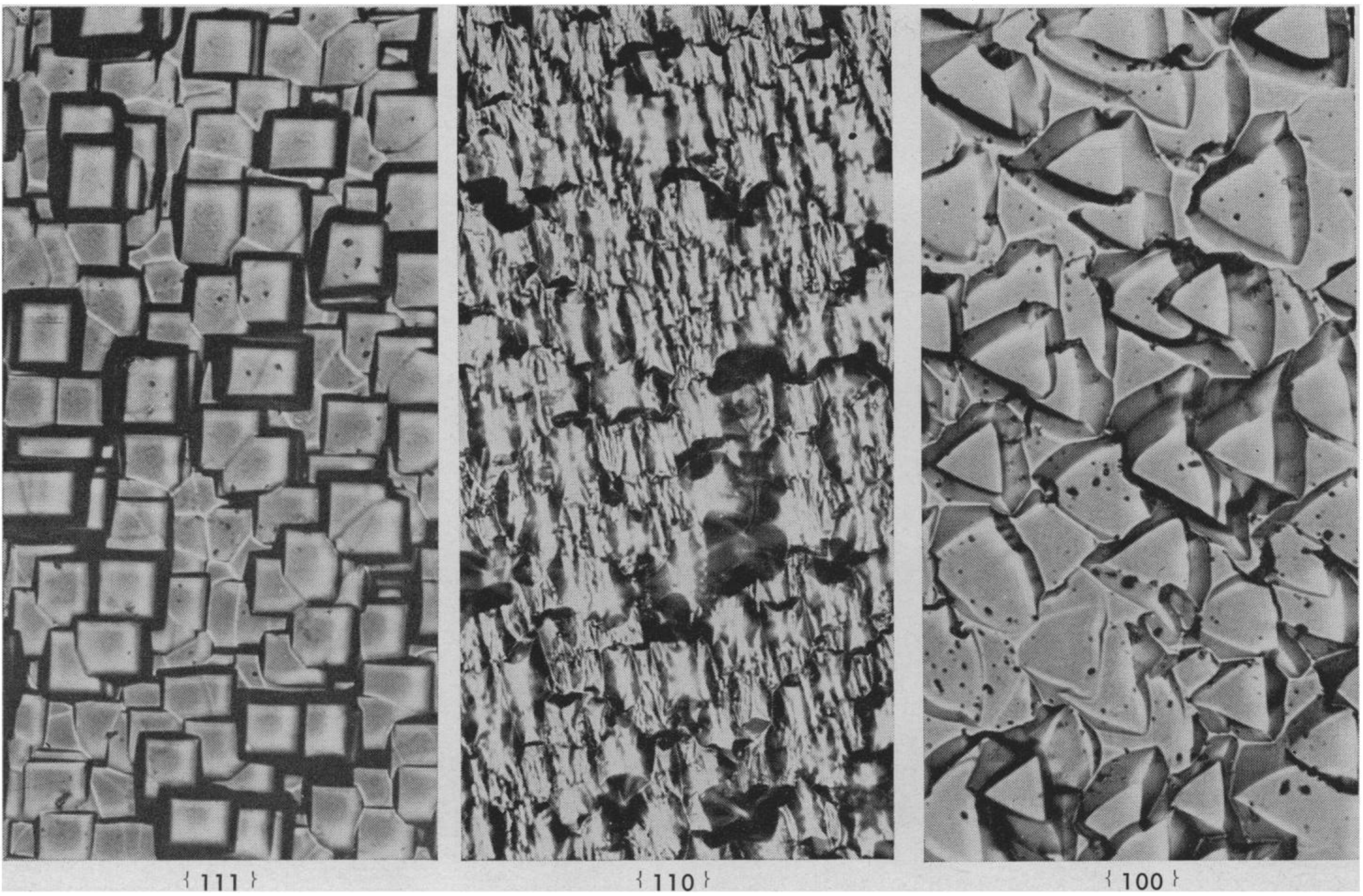
$\{111\}$ $\{110\}$ $\{100\}$

Fig. 2. Etch figures on the three main crystallographic planes of germanium. The symmetry of the corresponding crystallographic axis in the cubic system is clearly revealed. The etch figures have a threefold symmetry on the $\{111\}$ surface, twofold symmetry on the $\{110\}$ surface, and fourfold symmetry on the $\{100\}$ surface. The etch figures are composed of distinct crystallographic planes, which provide a useful criterion of relative crystallographic stability. Etchant, 30-percent H_2O_2 (1 part, by volume), 48-percent HF (1 part), and water (4 parts) (magnifications, from left: about 580, 1150, and 580).

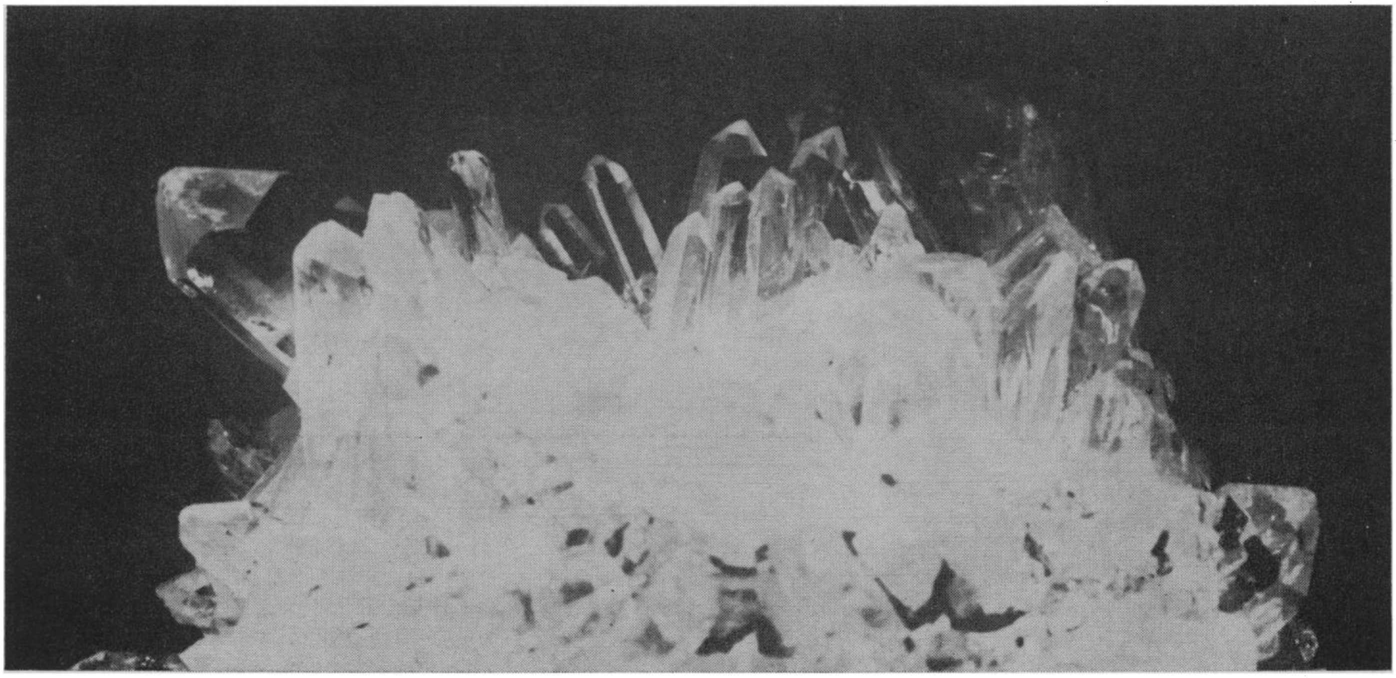

Fig. 3. Natural quartz crystals (hexagonal crystal class). The natural habit is apparent: hexagonal prisms elongated along the C axis.

nucleation and growth of crystals, and the effect of the crystalline structure of the substrate surface on the epitaxially grown layer is most striking.

4) Formation of surface layers of reaction products—for example, oxides. High-temperature oxidation in gaseous media is usually markedly dependent on orientation, so that at a certain stage in the oxidation process the variation of oxide thickness with orientation can be readily seen from interference colors (Fig. 5). Epitaxial growth is occasionally observed during oxide-layer formation.

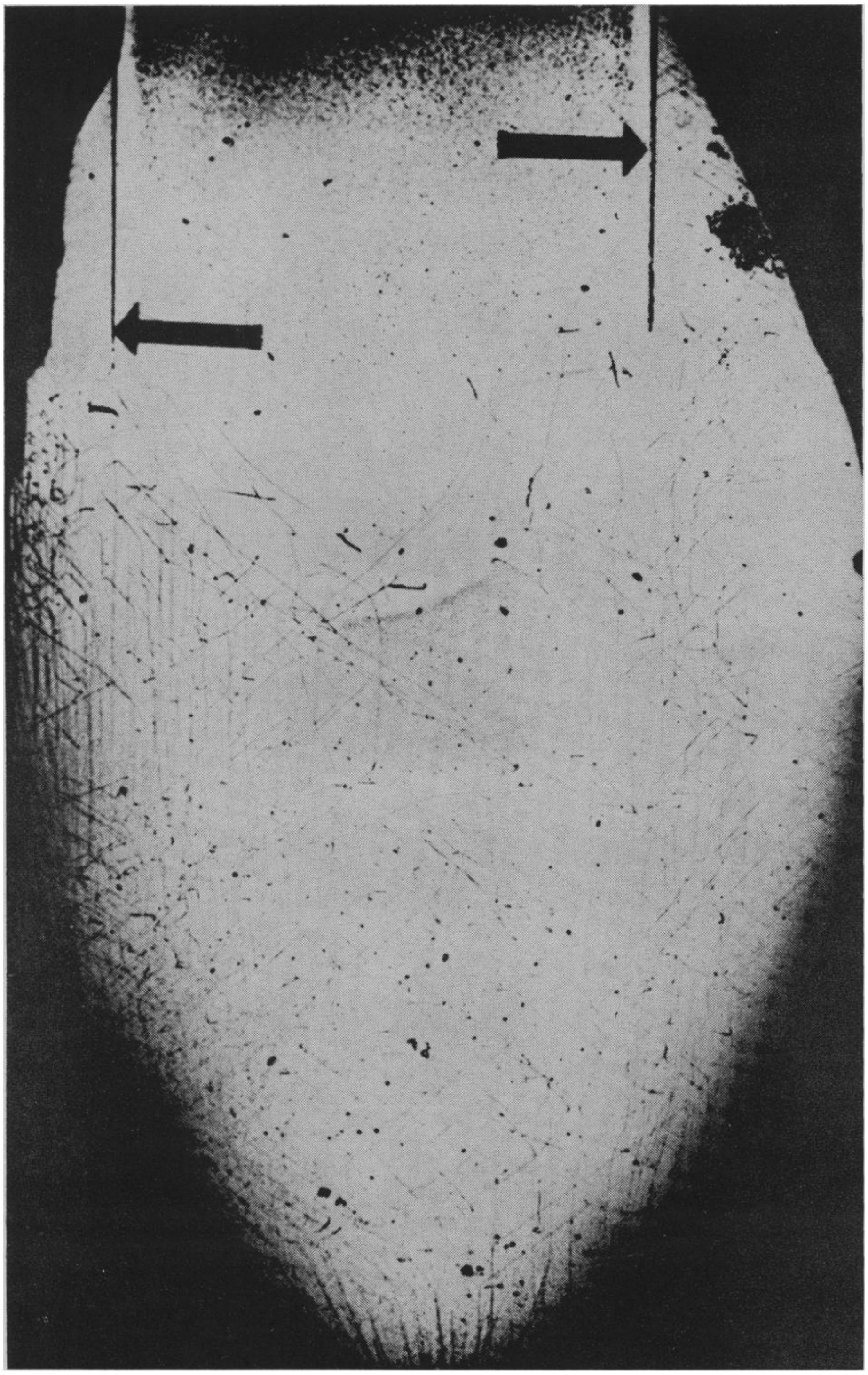

Fig. 4. A silicon crystal, showing a network of dislocations (revealed by decoration techniques). The arrows indicate the surface of the original silicon bar, onto which molten silicon was allowed to solidify. At the sides of the bar epitaxy was poor (for experimental reasons). In the region where epitaxy was good (the original interface cannot even be seen), a number of dislocations extend from the original bar into the new crystal. Additional dislocations are formed by thermal stresses (*11*).

Surface Configuration of Materials with Diamond Structure

The diamond-type elemental crystals, such as silicon and germanium, are characterized by four equivalent tetrahedral bonds resulting from the combination of the one *s* and the three *p* atomic orbitals (sp^3 hybridization); that is, if a given atom is visualized as being at the center of a tetrahedron, its four nearest neighbors are located at the corners. Termination of the lattice in a {111} plane gives rise to surface atoms each having a half-filled dangling orbital of one electron. The reactivity of a {111} surface can be related to the tendency of each of these dangling bonds to acquire a second electron. The atomic and electronic configuration of the principal crystallographic planes of the diamond-type crystals is shown schematically in Fig. 6. On the basis of the density of dangling bonds one can largely account for the surface behavior of, for example, germanium in aqueous media (Table 1), as well as for differences in work function (*12*) and adsorption characteristics as a function of orientation.

The tendency of dangling bonds to achieve more stable configurations is reflected not only in the chemical behavior of the crystal surface but also in the electronic properties. The *p*-type character (conduction via holes) of clean germanium surfaces is believed (*13*) to be the result of this tendency:

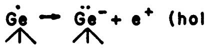

$$\underset{/|\backslash}{\dot{\mathrm{Ge}}} \rightarrow \underset{/|\backslash}{\ddot{\mathrm{Ge}}}^{-} + e^{+} \text{ (hole)} \qquad (1)$$

The hole (electron deficiency) shown in reaction 1 is a free positive carrier. The germanium atoms shown in the reaction are bonded to the lattice with three covalent bonds.

Similarly, specific adsorption of anions (X^-) on germanium may involve the formation of two-electron (covalent) bonds, as follows (*14*):

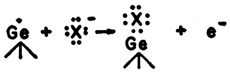

$$\underset{/|\backslash}{\dot{\mathrm{Ge}}} + :\underset{..}{\ddot{X}}:^{-} \rightarrow \begin{matrix} :\ddot{X}: \\ \ddot{\mathrm{Ge}} \\ /|\backslash \end{matrix} + e^{-} \qquad (2)$$

The electrons freed in reaction 2 result in an enhanced rate of dissolution and modify the effect of illumination on the electrode potential for germanium single crystals in aqueous solutions of surface-active anions (*15*).

In view of the tendency of the dangling orbitals to form covalent bonds, it is reasonable to ask why, upon exposure to adsorbing molecules, surfaces of covalent crystals do not become chemically inert. Although in some instances surfaces can become entirely inactive in the presence of adsorbing molecules, it is frequently observed that complete surface passivity cannot be induced, probably because stereohindrance or electrostatic forces, or both, prevent the formation of a continuous protective layer. Stereohindrance also appears to play an important role in determining the adsorption characteristics of the atoms of surface defects (for example, edge dislocations) (*16*). For reasons which are not understood at present, germanium surfaces are inert to water free of dissolved oxygen (*17*), although the reaction between germanium and water is thermodynamically possible:

$$\mathrm{Ge} + 2\mathrm{H_2O} \rightarrow \mathrm{GeO_2} + 4\mathrm{H^+} + 4e^- \qquad E^\circ = -0.15 \tag{3}$$

Traces of oxygen provide a kinetic path for the reaction through the formation of a water-soluble oxide.

To return to Fig. 6, it may be seen that the atoms of the {111} and the {110} surfaces have one dangling bond, whereas the atoms of the {100} surfaces have two dangling bonds. With regard to rearrangements of the surface atoms, one would expect the atoms of the {100} surfaces to exhibit the greatest tendency toward acquiring a more stable configuration. By employing low-energy electron diffraction techniques it was indeed found (*4*) that the relative positions of the atoms on clean {100} germanium surfaces (under high vacuum) are not the same as the positions on similar planes in the bulk crystal. Upon adsorption of oxygen, the rearrangement of the atoms can no longer be observed. Surface rearrangement is apparently of no particular significance in real surfaces.

The bonding configuration of the surface atoms may also account for the nucleation and crystal-growth characteristics of the principal crystallographic planes. The {111} surfaces do not favor nucleation. The first new atom to be added must form only one bond with a surface atom and remain with three dangling bonds. Thus, a monatomic layer cannot form on a {111} surface because a surface configuration with atoms having three dangling bonds is not stable. Nucleation and growth must proceed through diatomic layers (see Fig. 7, I). The probability of occurrence of such a process is relatively small. The {100} surfaces, where the surface atoms have two dangling bonds, favor nucleation and growth to a somewhat greater extent. In this case a new atom can form two bonds to the surface, one with each of two adjacent surface atoms, and thus remain with two dangling bonds. On the other hand, the atoms of the {110} surfaces have one dangling bond, one bond directed toward the interior of the crystal, and two bonds on the surface plane. It is apparent that the {110} surfaces favor the formation of monatomic layers and that nucleation is more likely to occur on these surfaces than on either the {111} or the {100} surfaces.

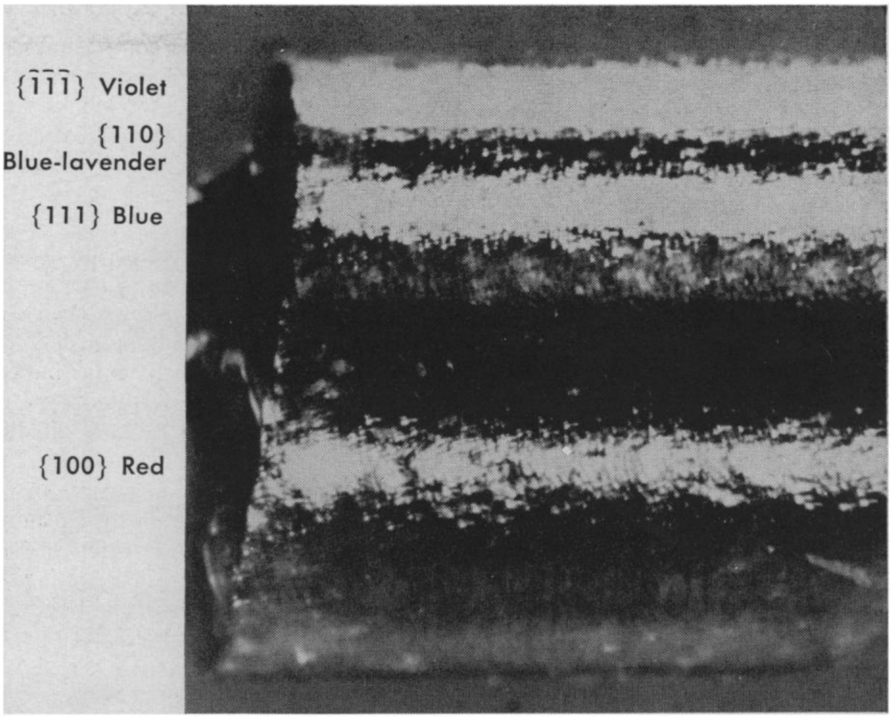

Fig. 5. A cylinder of indium antimonide (approximately 5 millimeters in diameter and 5 millimeters long), with its axis parallel to the < 110 > direction, oxidized in air at 350°C. A spectrum of colored bands was developed, reflecting the oxidation rates as a function of orientation. The relative rates of oxidation are as follows: $\{111\} > \{\bar{1}\bar{1}\bar{1}\} > \{110\} > \{100\}$. [See also Lavine, Rosenberg, Gatos, *J. Appl. Phys.* **29**, 1131 (1958)]

Bonding Model of the Surfaces of Intermetallic Compounds

Many binary intermetallic compounds are tetrahedrally bonded and have the zinc-blende structure, which is identical to the diamond structure except for the fact that zinc blende is made up of two kinds of atoms. Typical classes of compounds with the zinc-blende structure are the III–V compounds (for example, indium antimonide) and the II–VI compounds (for example, mercuric telluride). Some tetrahedrally bonded compounds, particularly of the II–VI type [for example, cadmium selenide (CdSe)] have the closely related wurtzite structure. The basic difference between the two structures is the stacking sequence of the atomic layers (Fig. 7). In the zinc-blende structure the atomic stacking pattern can be represented as A-B-C-A-B-C. . . . (cubic symmetry), whereas in the wurtzite structure the pattern is A-B-A-B. . . . (hexagonal symmetry). Both structures have two properties which make them ideally suited for studying the role of crystalline structure in surface reactivity: (i) they are covalently bonded, and (ii) they are noncentrosymmetric—that is, they exhibit crystallographic polarity in certain directions. The discussion which follows will be limited primarily to the {111} surfaces of the III–V compounds with the zinc-blende structure. The {100} and {110} surfaces are not so interesting, since the corresponding crystallographic directions are nonpolar.

As a consequence of the crystallographic polarity along the <111> direction of the zinc-blende structure, two types of {111} surfaces exist, one terminating with group III atoms (*18*) (A surfaces) and the other with group

V atoms (B surfaces), as shown in Fig. 7, I. The (111) surface on Fig. 7 cannot terminate with B atoms (white) because B atoms on the (111) surface would have three dangling bonds and only one bond to the lattice. This configuration is energetically unstable. For the same reason the $(\bar{1}\bar{1}\bar{1})$ surface cannot terminate with A atoms (black). It is not to be inferred from this reasoning that the $\{111\}$ and $\{\bar{1}\bar{1}\bar{1}\}$ surfaces are necessarily atomically flat, but rather that such surface steps as may exist must be diatomic or must be comprised of atoms in groups of some multiple of 2 (Fig. 8).

The electronic configurations of the $\{111\}$ surfaces are perhaps best visualized by considering a cut made perpendicular to the $<111>$ direction between planes AA and BB (Fig. 7, I) so that only one bond per atom is broken. Making the cut between planes AA and B′B′ involves the breaking of three bonds, a process requiring a great deal more energy. It is important to know how the two electrons comprising each bond being broken will be apportioned between the newly created surface atoms. In the case of the diamond-type crystals this question is easily answered: each atom will carry with it one electron of the cut bond.

The situation is different for the III–V compounds, however, since an isolated A atom has three outer-shell electrons and an isolated B atom has five. Simple chemical arguments indicate (*19*) that the surfaces created by a cut perpendicular to the $<111>$ direction will be as shown in Fig. 9—that is, the B surface has two electrons in the dangling bonds, while on the A surface there are no electrons which are not employed in bonding. Neglecting the partial ionic character of the bonds, we find that the electric dipoles at the two surfaces will be oriented as shown in Fig. 10 (*20*).

Chemical reactivities of the {111} surfaces. One would expect the A surfaces with no dangling electrons to be less reactive than the B surfaces toward oxidizing agents, which, by definition, accept electrons during reaction. Moreover, adsorption of electron donor molecules or negative ions should be stronger on the A surfaces than on the B surfaces, whereas the reverse should be found for adsorption of electron acceptors or positive ions.

Differences in chemical reactivity between the A and B surfaces were studied (*19*) by employing tetrahedral samples having exclusively A or exclusively B surfaces. The dissolution experiments showed that, in oxidizing media, B surfaces of InSb are markedly more reactive than A surfaces (*21*) (Fig. 11). It

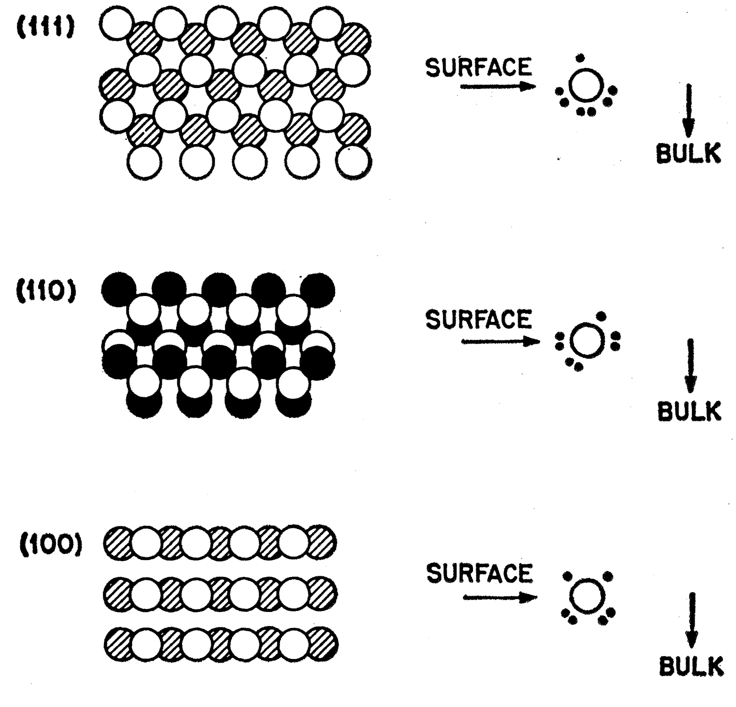

Fig. 6 (above). Structure of the $\{111\}$, $\{110\}$, and $\{100\}$ surfaces of the diamond-type crystals (germanium or silicon, for example) and the corresponding electron configuration of the surface atoms. In crystals with the zinc-blende structure (for example, indium antimonide), the plain and shaded atoms correspond to the group V and group III atoms, respectively. The electron configuration of the surface atoms of crystals of the zinc-blende type is not shown but is discussed in the text (*6*).

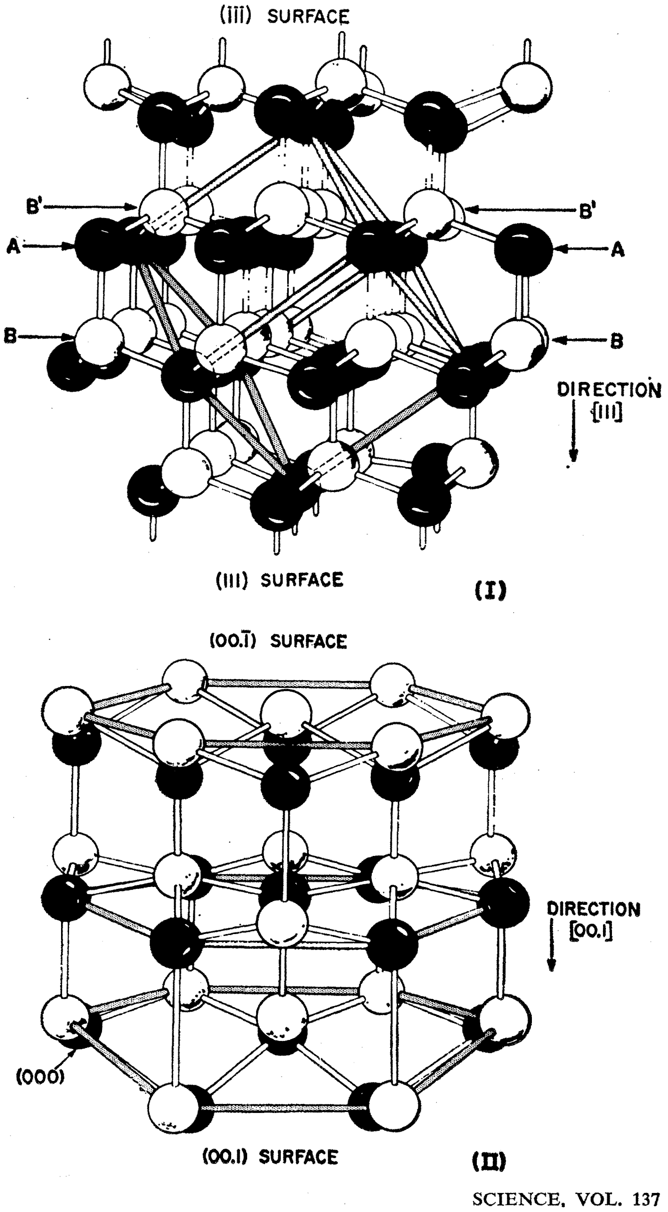

Fig. 7 (right). Models of the zinc-blende (I) and the wurtzite (II) structures. The corresponding cubic and hexagonal symmetries are clearly shown.

may be seen that at room temperature (or above) there is no difference in dissolution rate between the two types of surfaces, since the dissolution process is controlled by the transport of oxidizing species from the solution to the interface. Below room temperature, however, the dissolution of the A surfaces becomes activation-controlled, and differences in reactivity are then observed. It is important to note that, in studying orientation effects, the experimental conditions must be so chosen that the process under study is not under mass-transport control. Consistent with the results of Fig. 11, it was found (*19*) that in the same etching media the electrode potential of samples with exposed A surfaces was approximately 75 millivolts more noble than that of samples with exposed B surfaces (*22*).

These differences in dissolution rate may be readily understood, at least qualitatively (*21*), when it is recalled that dissolution of crystals proceeds through the propagation of atomic or molecular steps along the exposed surfaces (Fig. 8). The rate of motion of the diatomic steps (v_s) across the surface is a critical parameter in the dissolution process. It is reasonable to assume that atomic pits (created by the removal of one atom from layer I) or kinks (created by the removal of two adjacent atoms from layer I) are nucleation points for steps. The rate of nucleation of these defects (v_n) must be smaller than v_s, and, therefore, it constitutes the rate-determining step. If v_n were greater than v_s, a large number of atomic pits or kinks would be formed on the surface, leading to a surface configuration with both types of atoms; such a configuration is unstable, as I pointed out earlier. Therefore, the reactivity of the atoms in the outermost layer determines the overall chemical reactivity of the surface.

The dissolution rate of the B surfaces of InSb in an oxidizing etchant [70-percent HNO_3 (2 parts by volume), 48-percent HF (1 part), and glacial CH_3COOH (1 part)] at 0°C was decreased from 7.8 milligrams to 0.36 milligram per square centimeter per second in the presence of 0.5-percent butylamine (*21*). Other primary aliphatic amines gave similar results. However, no corresponding change in dissolution rate was observed for the A surfaces. It appears that the substituted ammonium ions

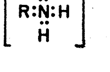

$$\left[\begin{array}{c}\mathrm{H}\\ \mathrm{R}:\!\overset{..}{\underset{..}{\mathrm{N}}}\!:\mathrm{H}\\ \mathrm{H}\end{array}\right]^{+}$$

adsorb preferentially on the B surfaces, which have a dipole moment, as indicated in Fig. 10, thereby decreasing the dissolution rate. Lack of inhibition in the case of the A surfaces reflects lack of significant adsorption of the species in question.

Structural properties. The B-surface atoms, with the two unshared electrons, can retain their sp^3 electronic configuration, much as nitrogen does in the ammonia molecule,

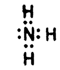

$$\begin{array}{c}\mathrm{H}\\ :\!\overset{..}{\underset{..}{\mathrm{N}}}\!:\mathrm{H}\\ \mathrm{H}\end{array}$$

with minor deviations from the tetrahedral symmetry. The situation is altogether different in the case of the A surfaces, where there are not enough sufficient electrons to fill four tetrahe-

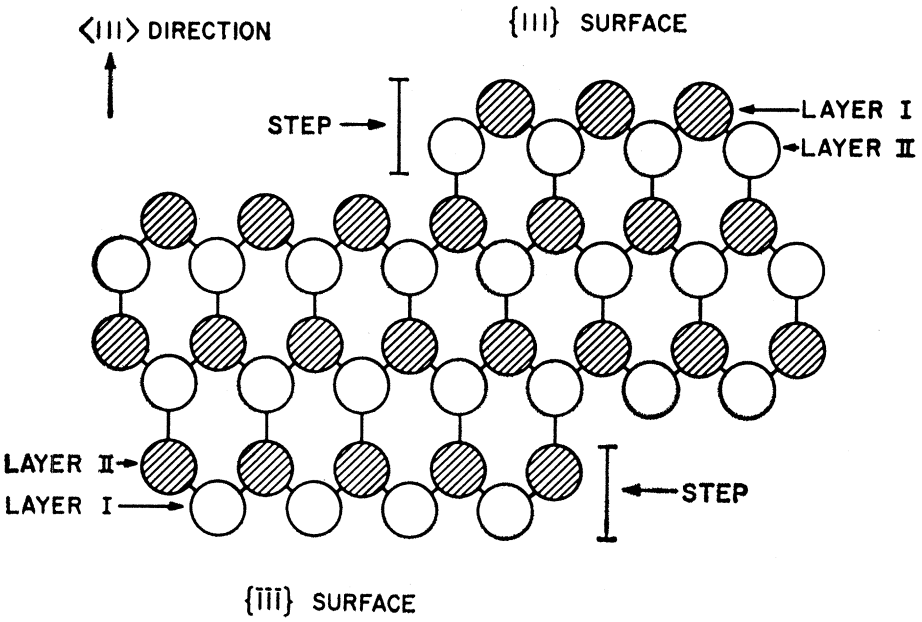

Fig. 8. Two-dimensional representation of the zinc-blende structure with diatomic surface steps (*21*).

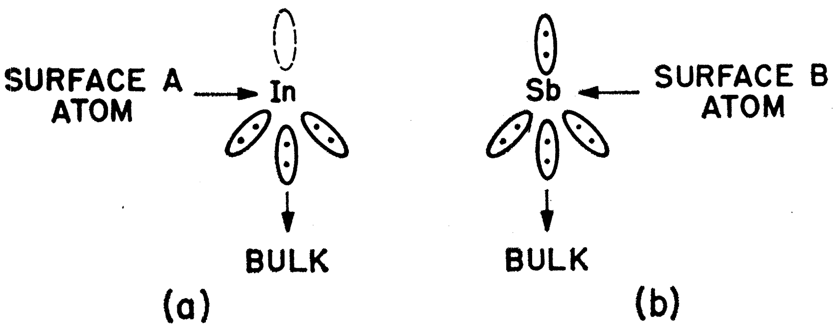

Fig. 9. Atomic model of the A and B {111} surfaces (*21*).

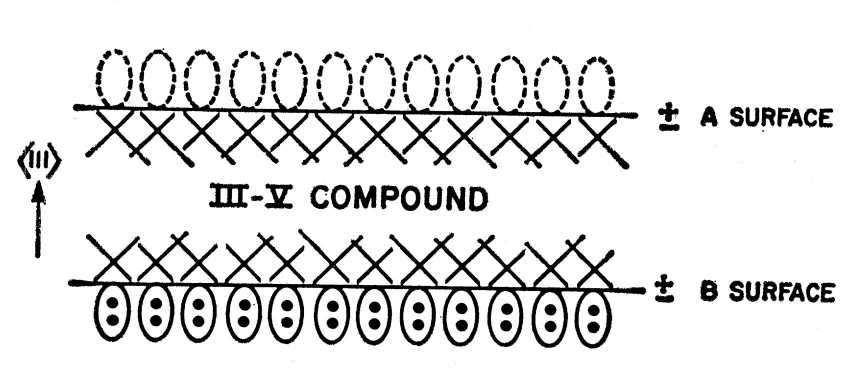

Fig. 10. Schematic representation of the dangling bonds on the A and B surfaces of III–V compounds and the associated surface dipole moment (*20*).

dral orbitals. Consequently, sp^3 hybridization cannot be maintained, and the angles of the three bonds to the lattice must be distorted. The bonds to underlying atoms presumably tend to become coplanar, as in many compounds of trivalent group III elements (for example, $InCl_3$). A planar configuration, however, is not possible, in view of the tetrahedral configuration of the bonds underneath the surface layer, as well as for steric reasons. Thus, distortion of the three bonds of A-surface atoms will lead to a bonding configuration between sp^3 and sp^2.

Although a precise determination of the energy associated with the distortion of the A surfaces cannot be made at present, it is reasonable to assume that this energy is a substantial fraction of the normal tetrahedral bond energy. On this basis one would also expect crystal growth to meet with greater difficulties in the A direction

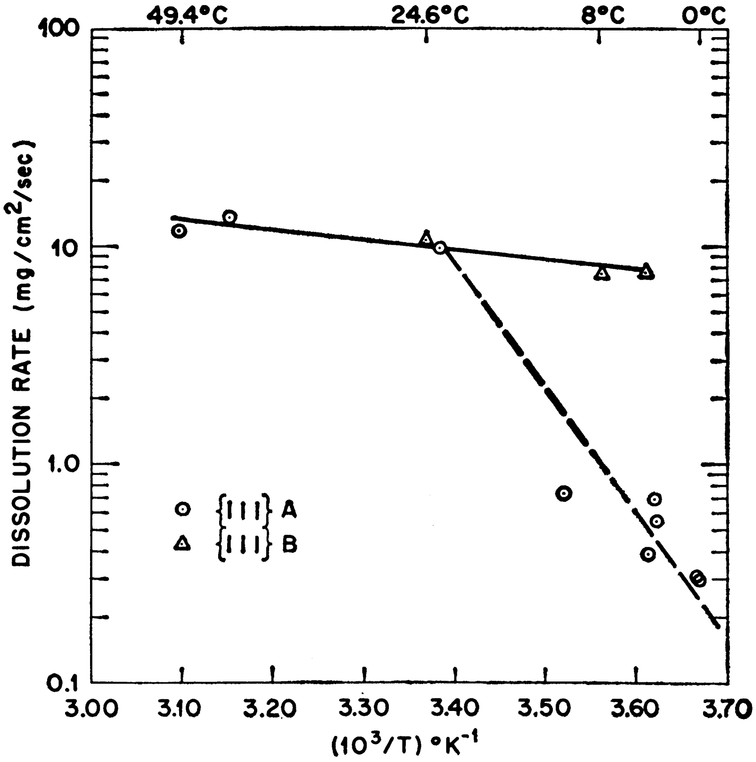

Fig. 11. Dissolution rate of indium antimonide as a function of temperature. Etchant, 70-percent HNO_3 (2 parts, by volume), 48-percent HF (1 part), and glacial CH_3COOH (1 part) (*21*).

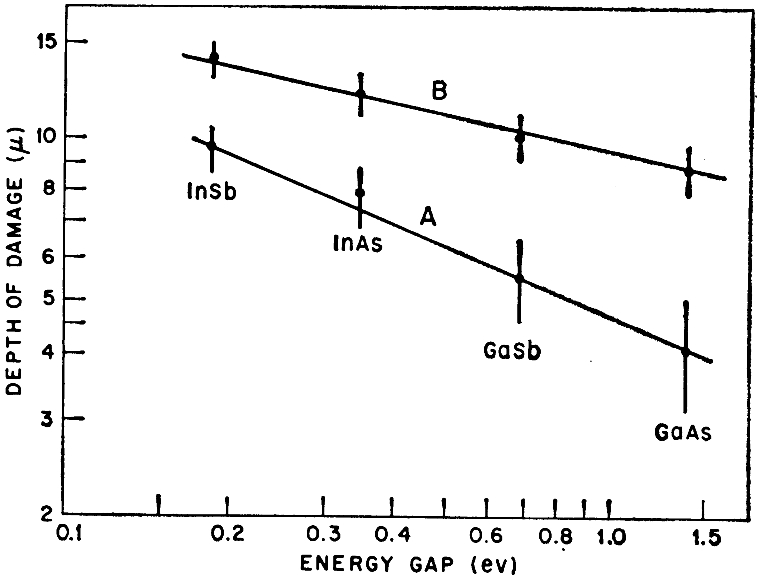

Fig. 12. Depth of damage in the A and B surfaces of III–V compounds as a function of energy gap. The surfaces were cold-worked with an abrasive of 20-micron particle size. [Gatos, Lavine, Warekois, *J. Electrochem. Soc.* **108**, 645 (1961)]

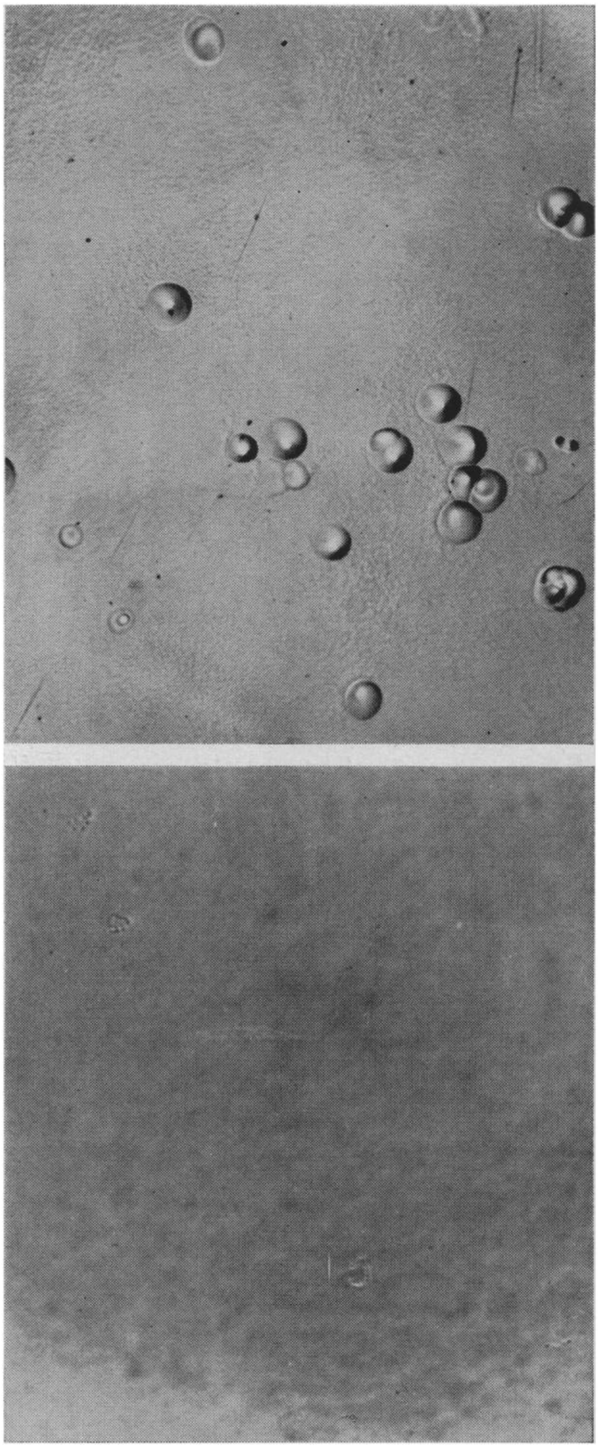

Fig. 13. The A surface (top) and the B surface (bottom) of a {111} indium antimonide wafer. Dislocation etch pits appear on the A surface but not on the B surface. Etchant, 70-percent HNO_3 (5 parts, by volume), 48-percent HF (3 parts), and glacial CH_3COOH (3 parts).

than in the B direction. By employing double crystal x-ray spectrometry, it was found that the half-breadth (a measure of crystalline perfection) of the rocking curves of the A surfaces was greater than that of the B surfaces (*23*). The ratios of the measured half-breadths for the A surfaces (ϵ_A) and B surfaces (ϵ_B) were as follows: for InSb, $\epsilon_A/\epsilon_B > 1.2$, and for GaAs, $\epsilon_A/\epsilon_B > 1.1$. The observed differences were well outside the limits of experimental error.

Consistent with this result was the finding that the cold work introduced by abrasion leads to a greater depth of damage in the B surfaces than in the A surfaces (Fig. 12). Furthermore, it was observed that crystal growth from the melt in the A <111> direction leads to a less perfect crystal (one of high dislocation density) than crystal growth in the B <111> direction (*24*). Actually, under the experimental conditions commonly employed, growth of single crystals in the A direction is extremely difficult.

All of these results are in accord with the proposed atomic model of the A and B surfaces and the predicted distortion of the bonds in the case of the A surfaces.

Behavior of edge dislocations. In the zinc-blende structure, slip occurs in the {111} planes along the <110> directions. The dislocation axis in this structure is parallel to the <110> direction and forms a 60° angle with the Burgers vector (the lattice translation, or slip vector). In view of the fact that slip will occur between {111} planes of atoms connected with single bonds, it can be shown that there are two types of edge dislocations; one consists of a row of triply bonded A atoms (α dislocations), the other consists of a row of triply bonded B atoms (β dislocations) (*25*). Dislocations of both these types intersect the A and the B {111} surfaces at an angle of 60° (*26*). The characteristics of the triply bonded A and B surface atoms should be reflected in the behavior of the α and β dislocations.

It was observed some years ago (*27*), that, in a number of oxidizing etchants, dislocation etch pits (*28*) develop only on the A surfaces of InSb and other III–V intermetallic compounds (Fig. 13). Subsequently, it was shown by de-

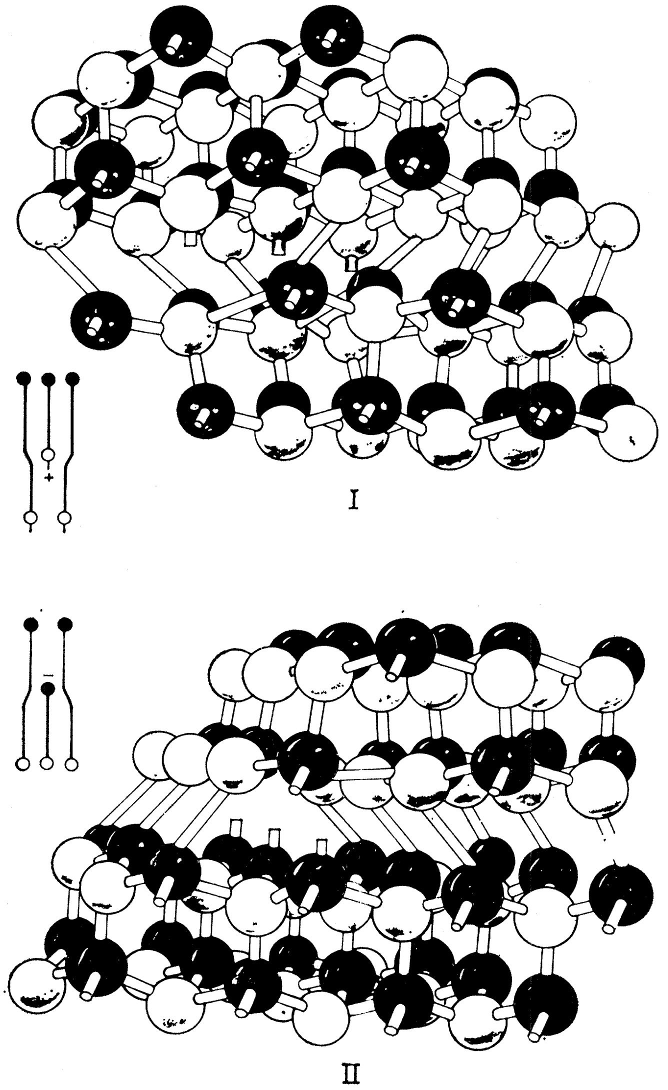

Fig. 14. Atom model, showing a 60° edge dislocation intersecting the A surface of a III–V compound. The surface of intersect is defined by the atoms with protruding bonds. (I) Dislocation with a row of B atoms; (II) dislocation with a row of A atoms (*19*).

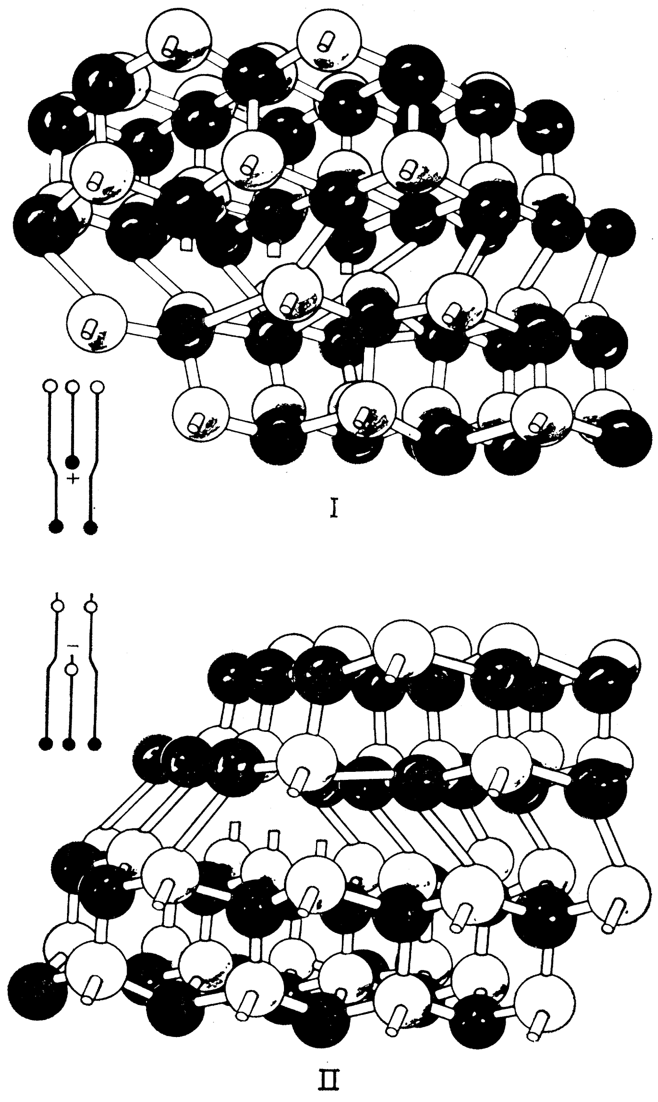

Fig. 15. Atom model, showing a 60° edge dislocation intersecting the B surface of a III–V compound. The surface of intersect is defined by the atoms with protruding bonds. (I) Dislocation with a row of A atoms: (II) dislocation with a row of B atoms (*19*).

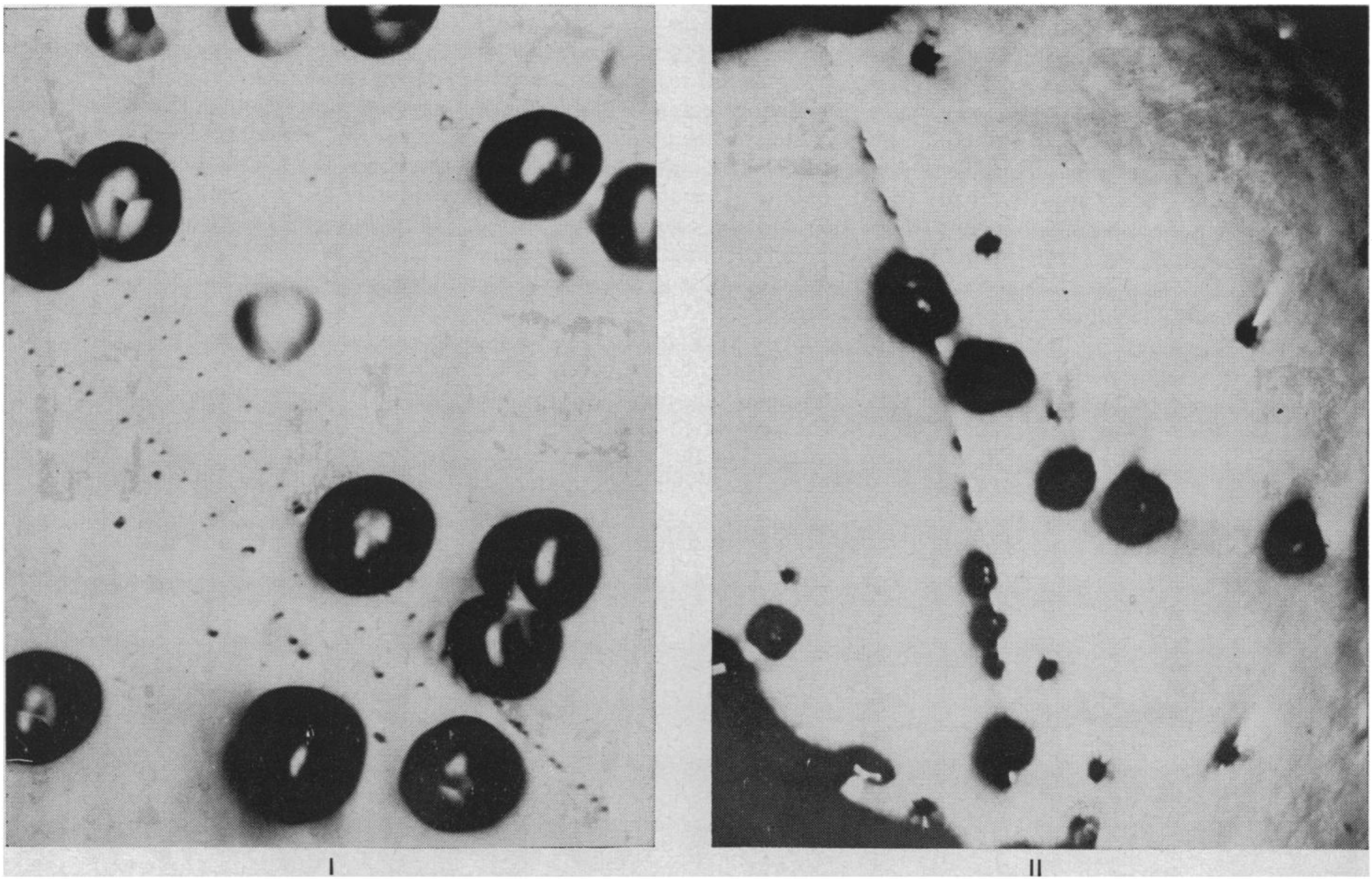

Fig. 16. Dislocation etch pits on the A (I) and B (II) surfaces of a $\{111\}$ wafer of indium antimonide. Two types of pits (very small and large) are apparent on the A surface. Etchant, 70-percent HNO_3 (2 parts, by volume), 48-percent HF (1 part), and glacial CH_3COOH (1 part). Temperature, 8°C. The etchant was saturated with stearic acid, which is slightly soluble (about × 45). [Gatos and Lavine, *J. Appl. Phys.* **31**, 743 (1960)]

formation experiments (*25*) that the etch pits on the A surfaces are associated with only one of the two types of edge dislocations. This result was rather surprising in view of the fact that the formation of dislocation etch pits had been generally attributed to enhanced chemical reactivity resulting from the lattice strain in the vicinity of the edge dislocations. According to that view, both types of dislocations should lead to the formation of etch pits, and on both types of $\{111\}$ surfaces. The experimental results, plus the fact that dislocations can also be revealed at low angle boundaries where they possess no additional lattice energy, indicate that the lattice strain associated with dislocations is not of primary importance in determining their increased chemical reactivity. For reasons which will become apparent, the III–V compounds are ideally suited for study of the chemical reactivity of dislocations and their role in surface reactivity.

The A and B surfaces were identified on an absolute basis by x-ray diffraction techniques (*29*). In the light of this identification and of the results of the deformation experiments on InSb (*25*), it was established (*19*) that the dislocation etch pits commonly formed on the A surfaces of III–V compounds are α dislocations. It is now possible to explain the formation of α-dislocation etch pits exclusively on the A surface solely on the basis of the proposed model for the triply bonded A and B surface atoms (including dislocation atoms), with the following straightforward assumptions: (i) The formation of a dislocation etch pit is the result of a greater rate of attack along the dislocation line than along the normal surface. (ii) The triply bonded B atoms are more reactive than the triply bonded A atoms toward oxidizing agents. (iii) Doubly bonded atoms are more reactive than triply bonded atoms.

Since both α and β dislocations intersect the A and B surfaces, there are four possibilities: Aα, Aβ (Fig. 14), Bα, and Bβ (Fig. 15). The chemical reactivity of each of these four surface-dislocation combinations are discussed in turn, with reference to Figs. 14 and 15.

Case Aα. The terminal doubly bonded A_2 (*30*) atom of the dislocation is the first one to be removed by reaction. This removal exposes two B_3 atoms, which will react more rapidly than the surface A_3 atoms. When these B_3 atoms react, four A_2 surface atoms are exposed, as well as an A_2 atom of the dislocation. Thus, the attack proceeds more rapidly along the dislocation than over the rest of the surface, and this leads to the formation of a dislocation etch pit.

Case Aβ. Strictly speaking, the terminal B_3 atom of the dislocation is not part of the outermost layer of surface atoms, and thus it would not be expected to initiate the etching process. However, if this B_3 atom is attacked prior to the attack of the A_3 surface atoms, then two A_2 surface atoms are exposed, leaving the next atom of the dislocation bonded to three A_3 atoms. It is apparent from Fig. 14 that the attack does not necessarily proceed preferentially along the dislocation but proceeds, rather, in a layer-like fashion over the surface.

Case Bα. This case is in many respects similar to the Aβ case. Actually, the conditions favor the formation of dislocation etch pits even less. The terminal atom of the dislocation is A_3, which is less reactive than the surface B_3 atoms.

Case Bβ. Although this case is the counterpart of Aα, it does not lead to the formation of dislocation etch pits. As the terminal dislocation atom B_2 is attacked, two A_3 atoms are exposed, and these will not react as fast as the B_3 surface atoms. These A_3 atoms delay exposure of the next B_2 dislocation atom until the surrounding B_3 surface atoms are attacked. Hence, no preferential attack along the dislocation axis takes place.

Altering of the surface and dislocation reactivity by adsorption. The explanation for the formation of α-dislocation etch pits on the A surfaces only is based on the fact that the triply bonded B atoms are more reactive toward oxidizing media than are the A atoms. Accordingly, by altering the relative reactivity of these atoms it should be possible to develop α- and β-dislocation etch pits on both the A and B surfaces. This has been accomplished by employing surface active agents which can adsorb preferentially on either the A or the B surface atoms.

The presence of aliphatic amines or aliphatic acids in oxidizing solutions leads to the formation of dislocation etch pits on the B surfaces (Fig. 16). The primary amines employed form positively charged ammonium ions in acid solution and adsorb preferentially (although not exclusively) on the B-surface atoms, as pointed out earlier. The resulting decrease in the reactivity of the B-surface atoms is responsible for the formation of pits on the B surfaces. The new etch pits are associated with β dislocations on the A surfaces and with α or β dislocations, or both, on the B surfaces.

By employing *n*-butylthiobutane in an oxidizing etchant [30-percent H_2O_2 (1 part, by volume), 48-percent HF (1 part), and water (8 parts)], dislocation pits were found on the A as well as on the B surfaces of InSb. However, it was shown that these pits do not correspond to the α-dislocation etch pits developed in the etchant that contained no butyl-

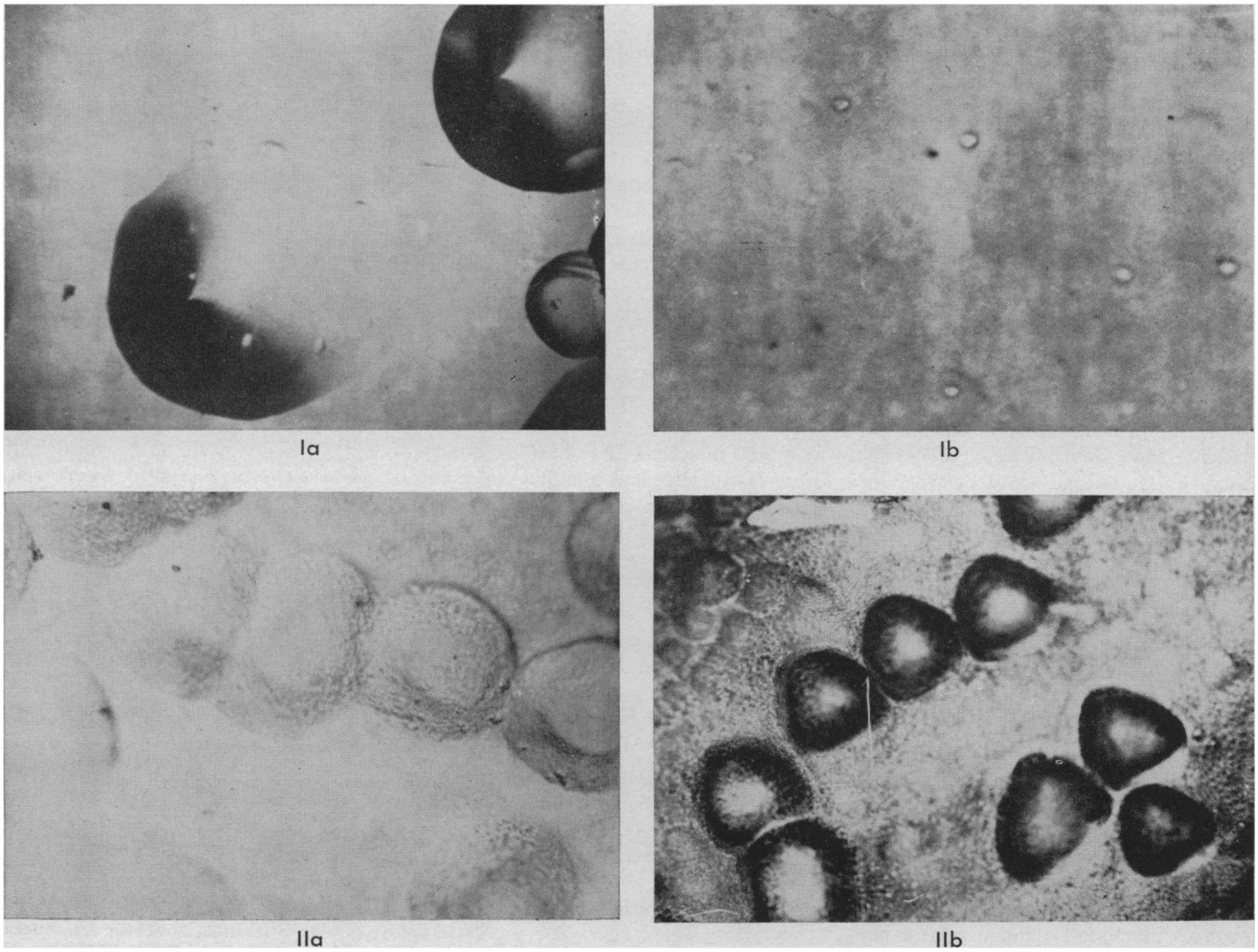

Fig. 17. The A and B surfaces of a { 111 } wafer of indium antimonide, Ia and Ib, respectively, etched in 30-percent H_2O_2 (1 part, by volume), 48-percent HF (1 part), and water (3 parts). These sample fields are parallel and corresponding. IIa and IIb are the A and B surfaces, respectively, in etchant containing the same components plus 0.4-percent butylthiobutane. It is clear that the dislocation pits formed in the two etchants do not correspond (about × 294). [From *16*]

thiobutane (Fig. 17). They are actually associated with β dislocations. This result must be attributed to the strong adsorption of the sulfoxide

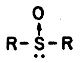

$$R-\overset{O}{\underset{\cdot\cdot}{S}}-R$$

formed by oxidation of the butylthiobutane, on the surface indium atoms, including the indium atoms at the intersection of the dislocation line with the surface.

The formation of β dislocation pits on the A and B surfaces of InSb can again be visualized with the help of the atom models shown in Figs. 14 (I) and 15 (II). In the case of the A surface the terminal dislocation atom A_3 lies in the layer below the indium surface atoms, which are also triply bonded. In the sulfide etchant, the room-temperature dissolution rate of the antimony surface is greater than that of the indium surface by a factor of more than 2 (*16*). Since the rate-determining step in the dissolution of the III–V compounds is associated with the reactivity of the outermost surface atoms, it must be concluded that here also the triply bonded B atoms are more reactive than the corresponding triply bonded A atoms. This difference in reactivity would favor attack along the β dislocation and would lead to etch-pit formation. In the case of the B surface, the terminal β dislocation atom is only doubly bonded and lies in the triply bonded outer surface layer. Thus, it will be the first to react, exposing adjacent triply bonded A atoms, which are less reactive than the triply bonded B atoms, as pointed out earlier. However, this would be the case only if the sulfoxide were to adsorb on the exposed indium atoms adjacent to the terminal dislocation atom. It is reasonable to believe that effective adsorption on these recessed atoms is not probable because of steric hindrance. Thus, dissolution along the dislocation in this case would proceed more nearly at the rates found in the absence of the sulfide. Indeed, the pits on the antimony surface are deeper than those developed on the indium surface by at least a factor of 2.

The association of certain pits with α dislocations and of others with β dislocations has been unambiguously confirmed by plastic deformation experiments (*16*). In these experiments excess α or β dislocations were introduced near the neutral plane, according to the particular orientation of the sample employed. Further discussion of these experiments is beyond the scope of this article.

Electronic properties. B-surface atoms, with two unshared electrons, are expected to act as electron donors, whereas A atoms, with no dangling electrons, are expected to act primarily as acceptors.

Direct observation of differences in electrical behavior attributable to the acceptor and donor nature of the A and B surface atoms, respectively, presents serious experimental difficulties stemming from the necessity for working with clean surfaces. However, triply bonded A or B atoms are also present along the line of edge dislocations where contamination presents no problem. The electronic configurations of the atoms along the edge dislocations should be nearly identical to those of the corresponding surface atoms. Consequently, the electrical behavior of edge dislocations should be similar to that of triply bonded surface atoms. By employing single crystal samples of *n*-type InSb in which an excess of α or β dislocations had been introduced by plastic deformation, it was unambiguously shown that triply bonded B atoms act as electron donors, whereas triply bonded A atoms act as electron acceptors (*31*).

Summary

The role of crystalline structure in the surface reactivity of predominantly covalent materials has been examined in terms of chemical bonding concepts. In this context a solid surface can be viewed as a giant lattice defect characterized by dangling bonds. Although it is difficult, at the present stage of development of the quantum mechanical approach to surfaces, to define precisely the perturbations resulting from the abrupt termination of the lattice at the surface, a host of experimental observations can be understood by assuming displacements of surface atoms and distortions of bonding configurations in accordance with simple chemical bonding principles.

A purely atomistic approach has been shown to account not only for the chemical behavior but also for certain structural and electrical characteristics of the surfaces considered. A number of phenomena, such as crystal growth and the behavior of certain lattice defects (for example, dislocations), are intimately related to the presence of dangling bonds and the associated distortions of the lattice at the surface (*32*).

References and Notes

1. I. Tamm, *Physik. Z. Sowjetunion* **1**, 733 (1932).
2. J. Bardeen, *Phys. Rev.* **71**, 717 (1947).
3. H. J. Juretschke, in *Surface Properties of Metals and Semiconductors*, H. C. Gatos, Ed. (Wiley, New York, 1960), p. 38.
4. R. E. Schlier and H. E. Farnsworth, in *Semiconductor Surface Physics*, R. H. Kingston, Ed. (Univ. of Pennsylvania Press, Philadelphia, 1957), p. 3.
5. See, for example, I. N. Stranski and R. Suhrmann, *Ann. Physik* **1**, 153 (1947).
6. H. C. Gatos, in *Surface Properties of Metals and Semiconductors*, H. C. Gatos, Ed. (Wiley, New York, 1960), p. 381.
7. See, for example, G. L. Kehl, *The Principles of Metallographic Laboratory Practice* (McGraw-Hill, New York, ed. 3, 1949).
8. A. P. Honess, *The Nature, Origin and Interpretation of the Etch Figures on Crystals* (Wiley, New York, 1927).
9. H. E. Buckley, *Crystal Growth* (Wiley, New York, 1951), p. 339.
10. H. Lassen, *Physik. Z.* **35**, 172 (1934).
11. W. C. Dash, in *Growth and Perfection of Crystals*, R. H. Doremus, B. W. Roberts, D. Turnbull, Eds. (Wiley, New York, 1958), p. 361.
12. F. Allen, *Tech. Repts. Cruft Laboratory, Harvard University, No. 236* (1955).
13. P. Handler, in *Semiconductor Surface Physics*, R. H. Kingston, Ed. (Univ. of Pennsylvania Press, Philadelphia, 1957), p. 23.
14. W. W. Harvey and H. C. Gatos, *J. Electrochem. Soc.* **107**, 65 (1960).
15. ———, *J. Appl. Phys.* **29**, 1267 (1958).
16. M. C. Lavine, H. C. Gatos, M. C. Finn, *J. Electrochem. Soc.* **108**, 974 (1960).
17. W. W. Harvey and H. C. Gatos, *ibid.* **105**, 654 (1958).
18. In the III–V compounds it is customary to designate the group III atoms as A atoms and the group V atoms as B atoms, in accordance with the often used notation $A^{III}B^{V}$. This is the designation used in this article.
19. H. C. Gatos and M. C. Lavine, *J. Electrochem. Soc.* **107**, 427 (1960).
20. H. C. Gatos, *J. Appl. Phys.* **32**, 1232 (1961).
21. ——— and M. C. Lavine, *J. Phys. Chem. Solids* **14**, 169 (1960).
22. The electrode potential during dissolution in oxidizing agents approaches the reversible potential of the electrode, so that a more noble dissolution potential is indicative of a lesser tendency of the material to react.
23. H. C. Gatos, M. C. Lavine, E. P. Warekois, *Proceedings of the International Conference on Semiconductor Physics, Prague* (1960), p. 519.
24. P. L. Moody, H. C. Gatos, M. C. Lavine, *J. Appl. Phys.* **31**, 1696 (1960).
25. J. D. Venables and R. M. Broudy, *ibid.* **29**, 1025 (1958).
26. The various types of dislocations proposed for the diamond-type structures [see J. Hornstra, *J. Phys. Chem. Solids* **5**, 129 (1958)] are not discussed here.
27. H. A. Schell, *Z. Metallk.* **48**, 158 (1957); J. W. Allen, *Phil. Mag.* **2**, 1475 (1957).
28. The association of etch pits with edge dislocations can be verified by various methods, one of which consists in following the dislocation line into the bulk by successive etchings.
29. E. P. Warekois and P. H. Metzger, *J. Appl. Phys.* **30**, 960 (1959).
30. The subscripts designate the number of covalent bonds to the lattice.
31. H. C. Gatos, M. C. Finn, M. C. Lavine, *J. Appl. Phys.* **32**, 1174 (1961).
32. I wish to thank H. H. Ehlers for preparing several of the photographic illustrations and Dr. W. W. Harvey for many profitable discussions. Lincoln Laboratory is operated with support from the U.S. Army, Navy, and Air Force.